Method to identify time delay of chaotic semiconductor laser with optical feedback

Yuanyuan Guo (郭园园), Yuan Wu (武 媛), and Yuncai Wang (王云才)*

Institute of Optoelectronic Engineering, College of Physics and Optoelectronics,

Taiyuan University of Technology, Taiyuan 030024, China

**Corresponding author: wangyc@tyut.edu.cn*

Received October 11, 2011; accepted January 10, 2012; posted online March 15, 2012

We propose a power spectrum analysis method to directly identify the time delay of a chaotic semiconductor laser with optical feedback. By measuring the radio frequency (RF) power spectrum of the chaotic laser and performing an inverse Fourier transform, we can easily unveil all the time delay signatures, regardless of whether the chaotic output is induced by single or multiple feedback. This method successfully retrieves the two time delay signatures from the power spectrum of a semiconductor laser with double-cavity feedback.

OCIS codes: 190.3100, 140.5960.

doi: 10.3788/COL201210.061901.

Optical chaos has attracted considerable attention in recent years due to its great applications in various fields, such as chaos-based communication encryption systems[1], chaotic lidars[2], fast random bit sequences generators (RNGs)[3], and chaotic optical time-domain reflectometry[4]. Through perturbing a semiconductor laser (SL) with optical injection, optical feedback, or optoelectronic feedback, the laser can be driven into broadband chaotic output[5]. Among the mentioned methods, the semiconductor laser with optical feedback (SL-OFB) may be the most common applied chaotic sources due to its unique virtues, such as simple configuration, small size, feasible controllability, and rich chaotic dynamics.

Nevertheless, the output of SL-OFB usually has periodic intensity fluctuations. These fluctuations are nearly identically repeated at the photon round-trip time in the external cavity, and are widely called the time delay (TD) signature. The TD signature seriously affects the performance of chaotic system in some applications. For example, the TD signature provides the clue to break the chaos-based secure communication and can deteriorate the randomness of RNGs based on SL-OFB. Some scenarios have been proposed to conceal the TD signature of SL-OFB. Typical scenarios are to generate high-dimensional chaos[6], to modulate the delay time[7,8], and to use multiple feedback[9,10]. Recently, Wu *et al.* experimentally showed that the TD signatures can be suppressed in two limits when double external cavities are used; one is that the two external cavities have roughly equal lengths, and the other is that one cavity length is approximately half of the other[11]. Rontani *et al.* proposed that TD signature identification would be impossible when the TD is close to the relaxation period of the laser operating with weak feedback[12]. Their theory was demonstrated experimentally in 2010[13].

In contrast, several techniques for extracting the TD signature also exist; however, usually, their observables are the recorded chaotic time series. Two widely applied techniques are the autocorrelation function (ACF) and the delay mutual information (DMI)[14]. Other techniques include the phase information[15], the minimal forecast error[16], the filling factor analysis[17], the permutation-information theory[18], and the extrema interval analysis[19]. In 2010, we found that the TD signature could be identified through observing the RF power spectral and observing its fine structure[20]. In this letter, we develop our earlier technique by combining the power spectrum analysis with inverse fast Fourier transform (IFFT) function. The results demonstrate that the TD signatures of the SL-OFB can be easily identified with our proposed method, even in cases where researchers claim that the ACF method failed to extract the TD[11−13].

Figure 1 shows the schematics of the experimental setup. A distributed feedback SL (DFB-SL) was used to generate chaotic light under single or dual external-cavity feedback. The DFB-SL was biased at 33.0 mA (approximately 1.5 I_{th}) by an ultralow-noise current source. Its temperature and wavelength were stabilized by a thermoelectric controller. Under these conditions, the lasing wavelength of the DFB-SL was measured to be approximately 1 554 nm and output power P_0 was approximately 1.1 mW with a relaxation oscillation approximately 3 GHz. The laser output was split into four parts by two fiber couplers (FC_1 and FC_2). The double external cavities were formed using fiber mirrors (FM_1 and FM_2). The two reflected beams by FM_1 and FM_2 were re-injected into SL. The intensity of the feedback light was adjusted by the variable optical attenuators (VOA_1 and VOA_2), respectively. An optical power meter (OPM) was used to monitor the power of feedback light (P_1) through a 30/70 fiber coupler (FC_1). The optical isolators (OI) were used to prevent the unwanted back-reflected disturbance from the front face of signal

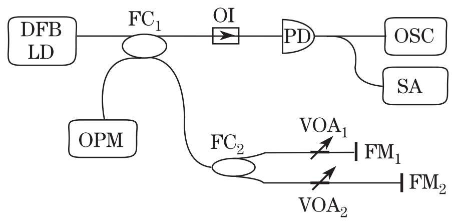

Fig. 1. Experimental setup for time delay identification.

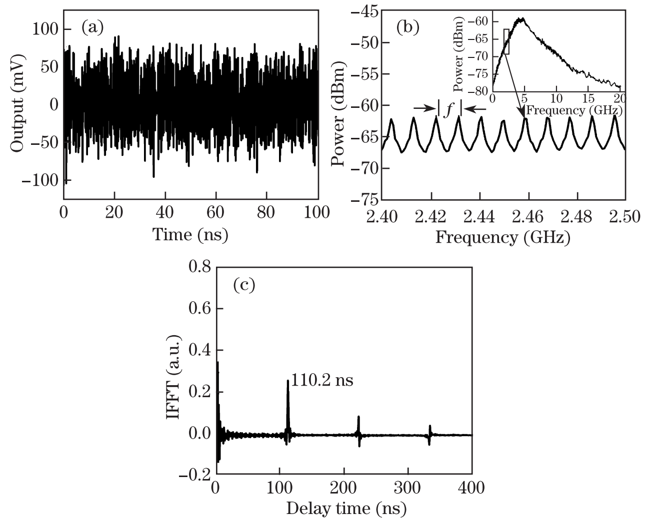

Fig. 2. Measured chaotic time series associated the local RF spectrum, and its inverse Fourier transform curve with single external cavity for L=11.02 m.

detection part. In the signal detection, the optical signal was transformed into electronic signal by a 47-GHz photodetector (PD, u2t, XPDV2020) and then analyzed by a digital oscilloscope (OSC) and a radio frequency (RF) spectrum analyzer. In our experiment, the feedback power ratio (FPR) is defined as the ratio of reflected power and the SL output power, FPR=P_1/P_0. The resonance frequency of the external cavity satisfies f=$c/2nL$, where L is the external cavity length, c is the light speed, and n is the fiber refractive index of 1.5. Clearly, the TD of τ is the reciprocal of f.

Firstly, we demonstrated how to identify directly the TD signature by locally enlarging the RF spectrum in the single external cavity scenario. Here, we took external cavity of L=11.02 m as an example, which corresponds to a resonance frequency of f=9.07 MHz (i.e., a TD of τ=110.2 ns). In the experiment, the FPR was 0.0178. Figure 2 illustrates the typical chaotic intensity time series and the power spectra of chaotic signal measured by the RF spectrum analyzer. The chaotic time series (Fig. 2(a)) behaved intricately and irregularly. The inset of Fig. 2(b) shows the whole RF power spectrum recorded by the RF spectrum analyzer. By enlarging a section of the RF power spectrum around the laser relaxation oscillation frequency, Fig. 2(b) shows that the spectrum is actually modulated in the resonance frequency of the external cavity of f=9.07 MHz. This phenomenon indicates that the TD can be extracted with ease by enlarging the RF power spectrum. To extract the delay more directly, we processed the RF spectrum with IFFT. The associated curve is shown in Fig. 2(c). The IFFT is defined as IFFT $(\tau)=\int P(f)\exp(j2\pi f\tau)\mathrm{d}f$, where $P(f)$ is the power spectral density of chaotic light measured by the RF spectrum analyzer and IFFT (τ) is the inverse

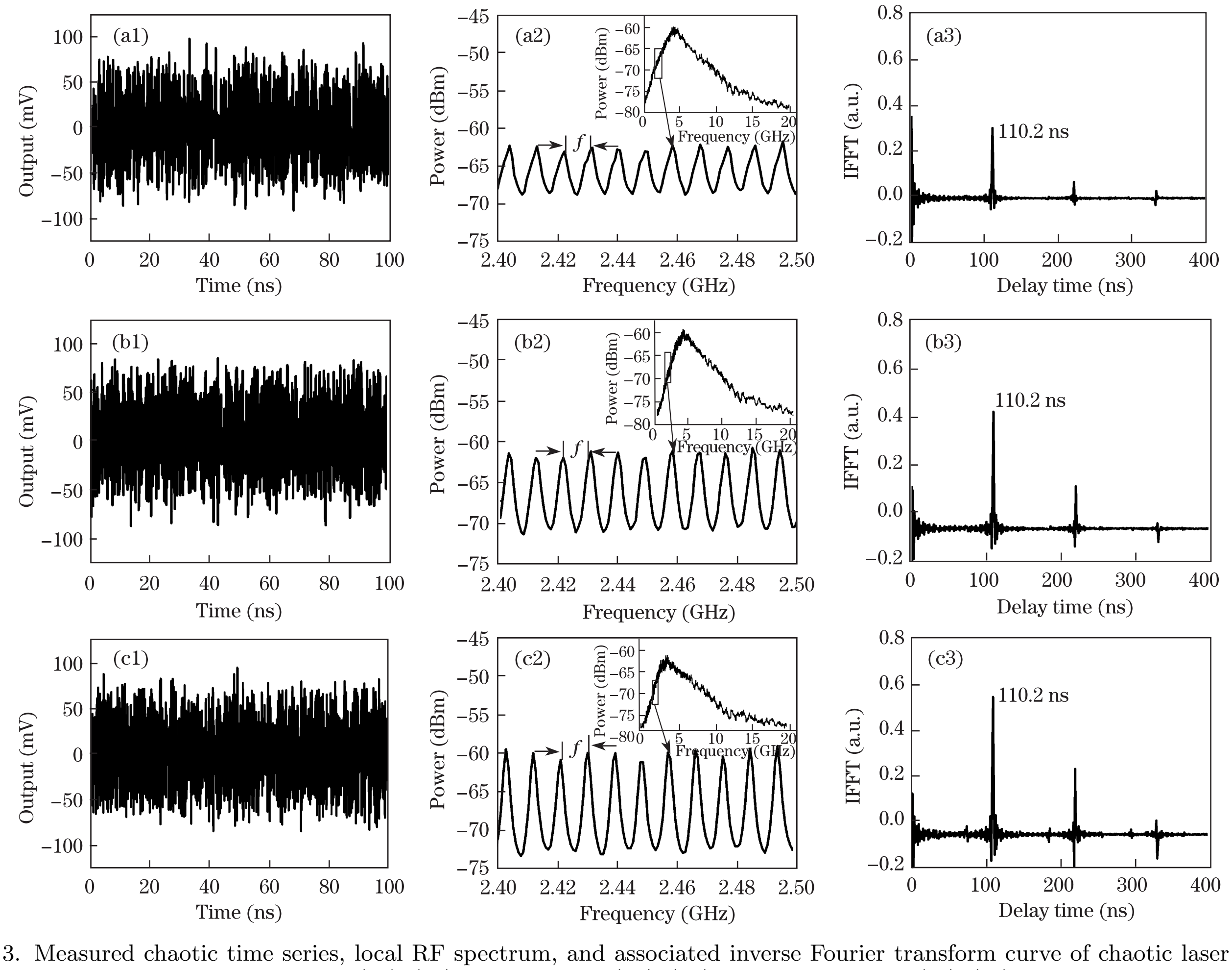

Fig. 3. Measured chaotic time series, local RF spectrum, and associated inverse Fourier transform curve of chaotic laser with single external cavity for L=11.02 m. (a1)–(a3) FPR=0.0185, (b1)–(b3) FPR=0.0127, and (c1)–(c3) FPR=0.0089.

fast Fourier transform function computed from the power spectral density. The location of a significant peak in IFFT curve corresponds to the TD signature of τ=110.2 ns. The above phenomenon is a universal existence observable with different RF spectrum analyzers (Agilent E4447A, Instek GSP-830E, and HP 8563E).

Meanwhile, we noted that the external feedback strength has no influence on the TD identification with our technique in single external cavity feedback. Figure 3 shows three sets of arbitrarily measured chaotic intensity time series, corresponding to the enlarged section of RF spectrum and IFFT curve with f=9.07 MHz and τ=110.2 ns for different values of FPR. Figure 3 shows that the external cavity can still be extracted easily utilizing the method above; however, FPR has been decreased greatly from 0.0185 to 0.0089. Moreover, the identification of TD signature becomes easier when the external feedback strength becomes very weak.

The small sensitivity described above may be because the time delay is very far from the relaxation time. Limited by experimental conditions, we numerically studied only the scenario where the time-delay is close to the relaxation time and the feedback intensity is sufficiently weak. The SL-OFB system can be modeled by Lang-Kobayashi rate equations:

$$\frac{\mathrm{d}E(t)}{\mathrm{d}t} = \frac{1}{2}(1+\mathrm{i}\beta)[G(t)-\gamma_{\mathrm{p}}]E(t) + \frac{\kappa_{\mathrm{cav}}}{\tau_{\mathrm{L}}}E(t-\tau_{\mathrm{cav}})\mathrm{e}^{\mathrm{i}2\pi\omega_0\tau_{\mathrm{cav}}}, \quad (1)$$

$$\frac{\mathrm{d}N(t)}{\mathrm{d}t} = J - \frac{N(t)}{\tau_{\mathrm{N}}} - G(t)\left|E(t)\right|^2, \quad (2)$$

where E is the slowly varying complex electric field, N is the average carrier density in the active region, and $G(\mathrm{t}) = g[N(\mathrm{t})-N_0]/[1+\varepsilon E(\mathrm{t})^2]$ is the gain coefficient. The following parameters are used in simulations: transparency carrier density N_0=0.455×10^6 μm^{-3}, differential gain g=0.85×10^{-3} μm^3·ns^{-1}, carrier lifetime τ_{N}=2 ns, photon lifetime τ_{p}=2 ps, round-trip time in laser intracavity τ_{L}=9 ps, linewidth enhancement factor β=5.5, gain saturation parameter ε=3×10^{-5} m^3, and angular frequency of SL ω_0=1.216×10^{-7}rad/s. Figure 4 shows the simulated results, including chaotic time series, autocorrelation function curve from the time series, RF spectrum, and the associated IFFT curve from the RF spectrum. In the simulation, the feedback strength k_{cav} was 0.05 and the TD was set as τ_{cav}=0.6 ns, which is approximately equal to the relaxation time of the chaotic laser (approximately 0.4 ns). Figure 4 shows that, although the TD was hardly identifiable by the ACF method (Fig. 4(b)), it could be obtained easily from the IFFT curve computed from the RF spectrum (Fig. 4(d)).

Secondly, we investigated the TD signatures in the double external cavities configure. We demonstrated that the TD signatures can also be directly extracted through enlarging the power spectrum of the chaotic laser, even when the lengths and FPRs of the two external cavities are rough equal and the difference of two delays is smaller than relaxation time of the laser. In our experiment, we fixed two external cavity lengths (L_1 and L_2) at 11.02 and 11.25 m, respectively, corresponding to the TDs of τ_1=110.2 and τ_2=112.5 ns ($\tau_1 \approx \tau_2$), respectively. Both the feedback power ratios (FPR$_1$ and FPR$_2$) were adjusted to 0.0171. The enlarged RF spectrum (Fig. 5(b)) showed that the RF power spectrum was modulated by the dual feedback; however, the identification of the TDs became difficult through observing the enlarged RF spectrum with naked eyes. Therefore, we plotted the IFFT curve of RF spectrum in Fig. 5(c), where the locations of two significant peaks corresponded to the TDs of τ_1=110.2 ns and τ_2=112.5 ns, respectively. Similar to the single-feedback situation, we further numerically studied the case where the difference between two similar TDs is smaller than the relaxation time. In our simulation, Eq. (1) was replaced by Eq. (3):

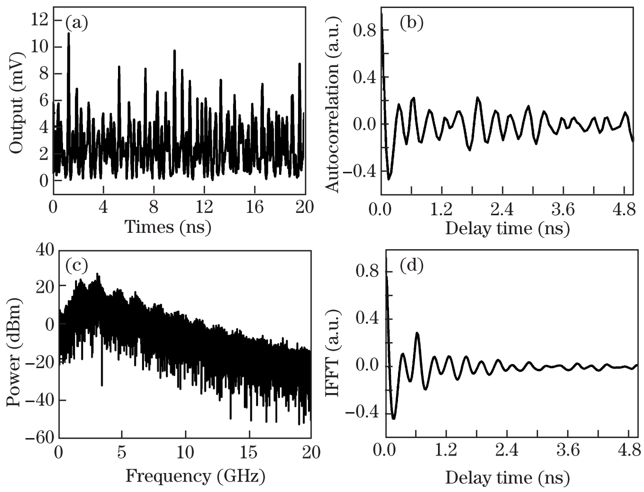

Fig. 4. Simulated results with single external cavity for τ_{cav}=0.6 ns and k_{cav}=0.05. (a) Chaotic time series, (b) autocorrelation function curve from the time series, (c) RF spectrum, and (d) the associated IFFT curve from the RF spectrum.

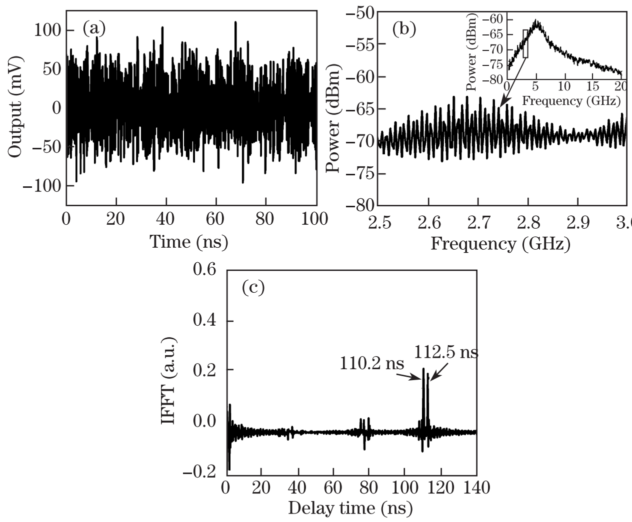

Fig. 5. Measured chaotic time series, local RF spectrum, and associated inverse Fourier transform curve of chaotic laser with dual external cavities for L_1=11.02 m and L_2=11.25 m.

$$\frac{\mathrm{d}E(t)}{\mathrm{d}t} = \frac{1}{2}(1+\mathrm{i}\beta)[G(t)-\gamma_{\mathrm{p}}]E(t) + \frac{\kappa_{\mathrm{cav1}}}{\tau_{\mathrm{L}}}E(t-\tau_{\mathrm{cav1}})\mathrm{e}^{\mathrm{i}2\pi\omega_0\tau_{\mathrm{cav1}}} + \frac{\kappa_{\mathrm{cav2}}}{\tau_{\mathrm{L}}}E(t-\tau_{\mathrm{cav2}})\mathrm{e}^{\mathrm{i}2\pi\omega_0\tau_{\mathrm{cav2}}}. \quad (3)$$

Here, the two feedback strengths are $k_{\mathrm{cav1}} = k_{\mathrm{cav2}}=0.05$ and the two TDs are set as $\tau_{\mathrm{cav1}}=3.1$ and $\tau_{\mathrm{cav2}}=3.25$ ns. Figure 6 shows the numerically obtained results. In this scenario, the TDs indeed cannot be extracted by the ACF method, as shown in Fig. 6(b), which is consistent with the report in Ref. [11]. However, two peaks are apparent in the IFFT curve from the RF spectrum (Fig. 6(d)), which correspond the two TDs. This result indicates that the TDs can still be retrieved successfully by our proposed method.

Finally, we demonstrated that, even if the two external cavities have arbitrary lengths, the TD signatures can still be identified with our technique. Here, we took a typical case for example. The two TD signatures were fixed at $\tau_1=112.5$ and $\tau_2=220.3$ ns (i.e., $\tau_2 \approx 2\tau_1$), respectively. The feedback power ratios were adjusted at $\mathrm{FPR}_1=0.0256$ and $\mathrm{FPR}_2=0.0133$. The chaotic time series, enlarged RF spectrum, and associated curve after the IFFT are illustrated in Fig. 7. In this case, the RF spectrum became very disorderly, as shown in Fig. 7(b); however, we could still identify the TD signatures of $\tau_1=112.5$ ns and $\tau_2=220.3$ ns by reading the locations of two significant peaks in the IFFT curve (Fig. 7(c)).

In fact, even if the difference of τ_2 and $2\tau_1$ is smaller than the relaxation time where the ACF method fails to extract the TD signature, it can still be easily identified using our method. We numerically studied this case in the model above, the simulation results are presented in Fig. 8. In our simulation, the two feedback strengths used were $k_{\mathrm{cav1}}=0.04$ and $k_{\mathrm{cav2}}=0.05$, whereas the corresponding two TDs were set as $\tau_{\mathrm{cav1}}=1.5$ ns and $\tau_{\mathrm{cav2}}=3.1$ ns. The autocorrelation curve (Fig. 8(b)) shows that the ACF can only distinguish one time delay (i.e., τ_{cav2}), which is consistent with the results obtained by Wu *et al*[11]. However, our method can identify both time delays simultaneously, as shown in Fig. 8(d). These results reveal that the second scenario in Ref. [11] is also not a sufficient condition for security.

In conclusion, we develope and demonstrate a practical method for TD signature identification in the chaotic laser with optical feedback. Using this technique, the TD signature can be directly retrieved by measuring the RF spectrum of chaotic laser and performing the IFFT on the locally enlarged RF spectrum. Even in some scenarios where previous studies show that the ACF method failed to extract TD signatures, our method can still identify the TD signatures successfully. The reason that earlier researchers are unable to obtain the TD signature in such scenarios by means of ACF method may be the shortage of recorded chaotic intensity time series and low sampling rates. Because the power spectrum of the chaotic light is modulated by the external feedback, we believe that the TD information of the chaotic laser with variable delays can also be extracted with our method.

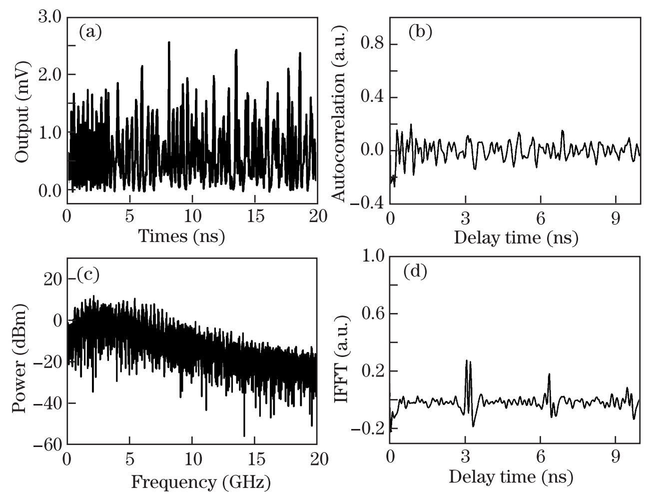

Fig. 6. Simulated results with two external cavities for $\tau_{\mathrm{cav1}}=3.1$ ns, $\tau_{\mathrm{cav2}}=3.25$ ns, and $k_{\mathrm{cav1}} = k_{\mathrm{cav2}}=0.05$. (a) Chaotic time series, (b) autocorrelation function curve from the time series, (c) RF spectrum, and (d) the associated IFFT curve from the RF spectrum.

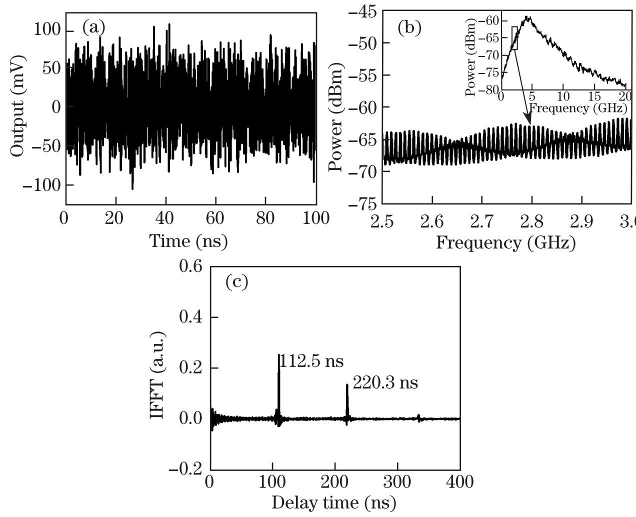

Fig. 7. Measured chaotic time series, local RF spectrum, and associated inverse Fourier transform curve of chaotic laser with dual external cavities for $L_1=11.25$ m and $L_2=22.03$ m.

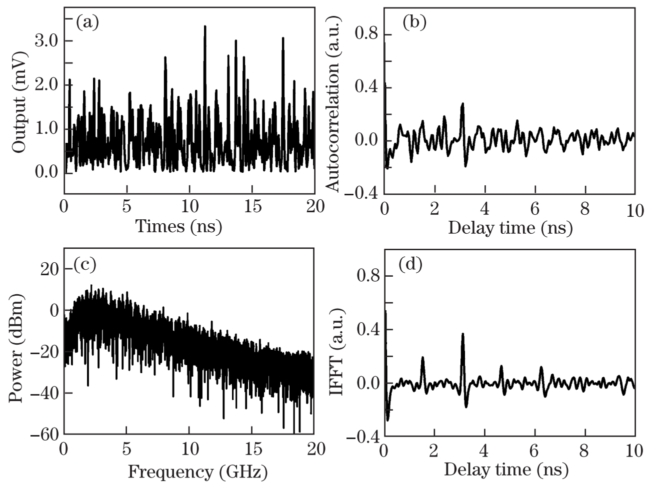

Fig. 8. Simulated results with two external cavities for $\tau_{\mathrm{cav1}}=1.5$ ns, $\tau_{\mathrm{cav2}}=3.1$ ns, $k_{\mathrm{cav1}}=0.04$, and $k_{\mathrm{cav2}}=0.05$. (a) Chaotic time series, (b) autocorrelation function curve from the time series, (c) RF spectrum, and (d) the associated IFFT curve from the RF spectrum.

This work was supported by the National Science Foundation for Young Scientists of China (Nos. 60908014, 60927007, and 61001114), the Natural Science Foundation for Young Scientists of Shanxi Province, China (No.

2009021003), and the Key Science and Technology Program of Shanxi Province, China (No. 20100321055-02).

References

1. A. Argyris, D. Syvridis, L. Larger, V. Annovazzi-Lodi, P. Colet, I. Fischer, J. García-Ojalvo, C. R. Mirasso, L. Pesquera, and K. A. Shore, Nature **437,** 343 (2005).
2. F. Y. Lin and J. M. Liu, IEEE J. Sect. Topics Quantum Electron. **10,** 991 (2004).
3. A. Uchida, K. Amano, M. Inoue, K. Hirano, S. Naito, H. Someya, I. Oowada, T. Kurashige, M. Shiki, S. Yoshimori, K. Yoshimura, and P. Davis, Nat. Photon. **2,** 728 (2008).
4. Y. Wang, B. Wang, and A. Wang, Photon. Technol. Lett. **20,** 1635 (2008).
5. A. Wang, Y. Wang, and J. Wang, Opt. Lett. **34,** 1144 (2009).
6. G. Perez and H. A. Cerdeira, Phys. Rev. Lett. **74,** 1970 (1995).
7. W. H. Kye, M. Choi, S. Rim, M. S. Kurdoglyan, C.-M. Kim, and Y. J. Park, Phys. Rev. E **69,** 055202 (2004).
8. R. M. Nguimdo, P. Colet, L. Larger, and L. Pesquera, Phys. Rev. Lett. **107,** 034103 (2011).
9. M. W. Lee, L. Larger, V. Udaltsov, E. Genin, and J. Goedgebuer, Opt. Lett. **29,** 325 (2004).
10. C. M. Kim, W. H. Kye, S. Rim, and S. Y. Lee, Phys. Lett. A **333,** 235 (2004).
11. J. Wu, G. Xiang, and Z. Wu, Opt. Express **17,** 20124 (2009).
12. D. Rontani, A. Locquet, M. Sciamanna, D. S. Citrin, and S. Ortin, IEEE J. Quantum Electron. **45,** 879 (2009).
13. J. Wu, G. Xia, X. Tang, X. Lin, T. Deng, L. Fan, and Z. Wu, Opt. Express **18,** 6661 (2010).
14. V. S. Udaltsov, J.-P. Goedgebuer, L. Larger, J.-B. Cuenot, P. Levy, and W. T. Rhodes, Phys. Lett. A **308,** 54 (2003).
15. R. M. Nguimdo, M. C. Soriano, and P. Colet, Opt. Lett. **36,** 22 (2011).
16. R. Hegger, M. J. Bünner, H. Kantz, and A. Giaquinta, Phys. Rev. Lett. **81,** 558 (1998).
17. M. J. Bünner, A. Kittel, J. Parisi, I. Fischer, and W. Elsäßer, Europhys. Lett. **42,** 353 (1998).
18. L. Zunino, M. C. Soriano, I. Fischer, O. A. Rosso, and C. R. Mirasso, Phys. Rev. E **82,** 046212 (2010).
19. B. P. Bezruckko, A. S. Karavaev, V. I. Ponomarenko, and M. D. Prokhorov, Phys. Rev. E **64,** 056216 (2001).
20. Y.-C. Wang, J.-S. Liang, A.-B. Wang, and M.-J. Zhang, Electron. Lett. **46,** 1621 (2010).